AO02 - Aerosol Inlet Design

Candidate 44263   Supervisor: Dr. Daniel Peters   Word Count:3812

Abstract

The efficiencies of various aerosol sampling systems are investigated drawing together both analytic and correlation equation soloutions from a variety of previous work and from this new sampling designs are suggested. A field test investigating the size distribution of tyre smoke aerosols from airplane landings is conducted using the suggested designs. No significant tyre smoke is observed despite the designs being sufficient for the task at hand.

1   Introduction

For the past few decades an important global concern has been the measurement of aerosols. Aerosols[1] have a dramatic effect on a wide range of situations.   One example very much in the publc eye at the moment is the greenhouse effect — tropospheric aerosols (such as anthropogenic sulthate) play a substantial role in the radiative forcing of global climate [4] or enhanced concentrations of sea salt can affect the global albedo [26], to cite but a few examples.

Aerosols can also have significant implications in industry and healthcare. The motivation behind the developments of new techniques and methods in aerosol measurement is twofold; firstly to guard the health of workers as required by law and secondly to aid productivity and thereby the competitiveness and efficiency of the company. Take the electronics industry as an example — in producing a semiconductior circuit board a single sub micrometer-sized particle can ruin the circuit if it sticks to the board where a sub micrometer circuit is to be laid [31]. The increasing importance of aerosol research is shown by the large number of aerosol research associations created in recent decades (including FAAM, AAAR and GAARA).

Many different instruments and techniques can be used to measure and catagorise properties of aerosols (e.g. a microcscope could be used to observe shape parameters or X-rays could be used to measure chemical properties). The issue that I will address is that of the sampling and transport of the aerosols from their natural location to a measuring instrument or collection bag.

The sampling of aerosols for accurate concentration and size distribution measurements is a non-trivial problem - this is the field of aerosol inlet design. For accurate measurements a representative sample of the aerosol must be drawn through an inlet and transported to the collection or measurement device.   In general, it is not possible to obtain information on particle size from the range $0.001\,\mu$m to $100\,\mu$m with a single instrument - this would be akin to using a $30\,$cm ruler to measure the length of a marathon route - so knowing the size cut offs of an inlet sampling system is an important part of aerosol measurement. There are many different factors which affect how representative a sampling system is from gravitational settling to inertial deposition on tube walls.

To achieve representative sampling the efficiency of the sampling system, which is governed by both inlet and transport line efficiency, must be known. Over the years, many different types of inlets have been designed including

---

[1]An assembly of liquid or solid particles suspended in a gaseous medium [31]

- Particle cup impactors [16] which remove larger particulates by their impact onto system walls

- Thin walled nozzles [1] where the ratio of external to internal diameter is less than 1.1

- Blunt samplers [30] where the inlet is small in comparison with the overall sampling diameter

- Sub-sampling systems [12] where isokinetic sampling[2] is achieved through the use of a large diameter primary sampler from which smaller inlets are used to take secondary samples

My research focused almost exclusively on thin walled nozzle systems as these are idealised sampling nozzles which do not disturb the ambient flow of gas and are therefore simpler to analyse. I also made a simple model of an existing sub-sampling system on the roof of the Oxford Atmospheric Physics building.

I am concerned with aerosol sampling efficiency, composed of the efficiency of both the inlet and the transport tube which include (but are not limited to);

- Angle of inclination of the inlet - determines the shape of the boundary layer inside the nozzle.

- Gravitaional settling - heavier particles are more likely to be deposited on the walls of the tube.

- Bend deposition - inertia causes particulates to deviate from the gas flow and impact on tube walls.

2 Methodology

Numerous papers exist on modelling the fluid dynamics of a gas flow in and around an aerosol sampling inlet and its transport tube. In order to create new inlet designs and calculate the efficiencies of existing inlets IDL [3] was used to compile programs which use existing analytic solutions and correlations as models. Unless otherwise stated all subsequent equations (which assume that the inlet is of the *thin wall* type) are incorporated into my model.

2.1 Inlet Efficiency

The four primary influences on inlet efficiency are the orientation to the direction of flow, ratio of ambient to inlet gas velocity[4], inlet length and inlet diameter. A sampling nozzle can be used in any orientation. Convention dictates that a nozzle is said to face in the opposite direction to the inlet sample flow direction (i.e. a nozzle which faces upwards draws a sample downwards) and a nozzle which faces into the gas flow is said to be isoaxial. Anisoaxial sampling occurs for nozzles inclined at an angle to the flow. (figure 1).

The efficiency of a thin walled nozzle can be divided into three catagories.

Aspiration Efficiency

Much research into the aspirational efficiency of an isoaxial sampling inlet system has been done. Liu, Zhang and Kuehn [19] have given an equation for efficiency based on numerical data:

$$\eta_{\text{asp}} = 1 + \frac{\frac{U_0}{U} - 1}{1 + \frac{0.418}{Stk}}, \frac{U_0}{U} > 1$$

---

[3]Interactive Data Language

[4]Sampling gas velocity should be low enough so that particulates drawn in can accommodate themselves to the inlet gas velocity in a short distance (comparable to the inlet length), whilst at the same time be great enough that particle settling velocities are small in comparison so that gravitational settling is not present.
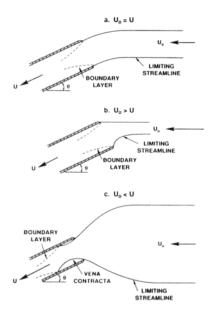
[2]A nozzle with sample flow speed (U) which matches the ambient gas velocity(U_0) is said to be isokinetic.

ANISOAXIAL SAMPLING

Figure 1: Schematic diagram of anisoaxial sampling with a thin walled nozzle. Sample flow velocity U, inclined at sampling angle θ and ambient gas velocity U_0. Reproduced from [31]

.

$$\eta_{\text{asp}} = 1 + \frac{\frac{U_0}{U} - 1}{1 + \frac{0.506(\frac{U_0}{U})^{0.5}}{Stk}}, \quad \frac{U_0}{U} < 1$$

for [5] $0.01 \leq Stk \leq 100$ and $0.1 \leq \frac{U_0}{U} \leq 10$. These correlations are very close to those of Belyaev and Levin [2] and are in good agreement with other research [18; 7].

Hangal and Willeke [32] surveyed the literature on anisoaxial sampling and performed experiments on the subject from which they established a database on anisoaxial sampling and thus various correlations. For aspiration efficiency they found that Durham and Lundgren [8] agreed with their data for sampling angles from $0 - 60^o$ with the ex-

[5] Stk is the Stokes number of a flow, defined as the ratio of particle stopping distance to characteristic dimension (here diameter of the nozzle).

pressions:

$$\eta_{\text{asp}} = 1 + \left(\frac{U_0}{U} \cos\theta - 1 \right)$$
$$\times \left(\frac{1 - (1 + [2 + 0.617\frac{U_0}{U}Stk']^{-1})^{-1}}{1 - (1 + 2.617Stk')} \right)$$
$$\times (1 - [1 + 0.55Stk' \exp^{0.25Stk'}]^{-1})$$

where $Stk' = Stk \exp^{0.022\theta}$

for $0.02 \leq Stk \leq 4$ and $0.5 \leq \frac{U_0}{U} \leq 2.0$. For $45^o \leq \theta \leq 90^o$ Laktionov's correlation [17] gives a good fit.

$$\eta_{\text{asp}} = 1 + \left(\frac{U_0}{U} \cos\theta - 1 \right)\left(3Stk^{(\frac{U}{U_0})^{0.5}} \right)$$

Transmission losses

Particulates can be deposited in the nozzle of the inlet by gravitational settling and by inertial effects.

Gravitational losses.

Many researchers (e.g. Okazaki, Wiener and Willeke [20]) use the criteria that if a particle penetrates the boundary layer formed at the entrance of the inlet (see figure 1) then it will be deposited by gravitational settling. Schlichting [27] gives that the boundary layer thinckness is characterised by the Reynolds number and the fraction of particles which penetrate into this layer is characterised by the Stokes number. From this we use the gravitational deposition parameter, $Z = (LV_{ts}/Ud)^6$, to characterise deposition in the boundary layer. It is the ratio of the particle settling distance during transport in the inlet region to the diameter of the inlet [31].

Experiments performed by Okazaki et al. [20] give the correlation for the gravitational transmission efficiency as:

$$\eta_{\text{trans,grav}} = e^{-4.7K^{0.75}}, \quad K = Z^{0.5}Stk^{0.5}\text{Re}^{-0.25}.$$

[6] L is inlet length, V_{ts} is the terminal settling velocity of the particulates.

Hangal and Willeke [32] again extended this work to account for nozzle inclination. For anisoaxial sampling they give:

$$\eta_{\text{trans,grav}} = e^{-4.7K_\theta^{0.75}}, \quad K_\theta = K(\cos\theta)^{0.5}.$$

Inertial losses.

From the examination of inertial losses at inlets Liu, Zhang and Kuehn [19] and Hangal and Willeke [32] give the following correlations for inertial transmission efficiencies:

$$\eta_{\text{trans,inert}} = \frac{1 + (\frac{U_0}{U} - 1)/(1 + \frac{2.66}{Stk^{2/3}})}{1 + (\frac{U_0}{U} - 1)/(1 + \frac{0.418}{Stk})},$$

for $0.01 \leq Stk \leq 100$ and $1 < \frac{U_0}{U} \leq 10$ and

$$\eta_{\text{trans,inert}} = e^{-75I_v^2}, \quad I_v = 0.09[Stk\frac{U - U_0}{U_0}]^{0.3},$$

for $0.02 \leq Stk \leq 4$ and $0.25 \leq \frac{U_0}{U} < 1.0$.

For anisoaxial inlets, Hangal and Willeke [32] give a correlation for losses in the vena contracta[7] and for losses from direct impaction with the wall of the nozzle. This is expressed as:

$$\eta_{\text{trans,inert}} = e^{-75(I_w + I_v)^2},$$

for $0.02 \leq Stk \leq 4$ and $0.25 \leq \frac{U_0}{U} < 4$. The vena contracta loss parameter is defined as

$$I_v = 0.09\left(Stk\cos\theta\frac{U - U_0}{U_0}\right)^{0.3}$$

for $0.25 \leq \frac{U_0}{U} \leq 1.0$ and $I_v = 0$ otherwise. The direct impaction loss parameter is defined as

$$I_w = Stk\left(\frac{U_0}{U}\right)^{0.5}\sin(\theta \mp \alpha)\sin\left(\frac{\theta \mp \alpha}{2}\right),$$

for upwards or downwards facing nozzles respectively.

$$\alpha = 12\left(1 - \frac{\theta}{90} - e^{-\theta}\right)$$

---

[7]See figure 1

2.2 Transport Line Efficiencies

The particulates, once sampled, must be transported to their ultimate destination (either a measuring or collection device) and losses occur during this transportation. My functions incorporate the biggest contributors to line losses - gravitational settling, diffusional deposition and inertial deposition at a bend. Both laminar and turbulent flow cases are considered.

Gravitational Settling

During transport particles settle and deposit on the walls of non vertical tubes due to gravitational forces. Fuchs [10] and Thomas [29] independantly solved gravitational settling problems by assuming a parabolic flow distribution. They produced an equation for transport efficiency for gravitational deposition for laminar flow in a circular, horizontal tube. This was later modified by Pich [22] to account for elliptical tubes. Further to this, Heyder and Gebhart [14] modified the equations to account for inclination of the tube to the horizontal. My investigations are solely concerned with circular tubes which are either horizontal or vertical for which the appropriate functions are:

$$\eta_{\text{tube,grav}} = 1 - \frac{2}{\pi}[2\varepsilon\sqrt{1 - \varepsilon^{2/3}} - \varepsilon^{1/3}\sqrt{1 - \varepsilon^{2/3}}$$
$$+ \arcsin(\varepsilon^{1/3})],$$
$$\varepsilon = \frac{3Z}{4} = \frac{3LV_{ts}}{4dU}.$$

In laminar flow in a vertical tube the Saffman force should also be considered[24; 25]. This is discussed by Grinshpun and Semenyuk [13] who come to the conclusion that the force is noticeably present for particles greater than 15 μm in diameter. I am mostly concerned with particulates smaller than 10 μm so I have assumed the Saffman force to be negligible in my calculations.

If the flow is turbulent Schwendiman et al. [28] gives the gravitational deposition efficiency of a

sample line as:

$$\eta_{\text{tube, grav}} = e^{\frac{-4Z}{\pi}} = e^{\frac{-dLV_{ts}}{Q}},$$

where Q is the volumetric flow rate of gas through the tube. Yamano and Brockmann [33] have also shown that turbulent flow through a bending tube has the same gravitational transport efficiency as a horizontal tube of the same diameter and length equal to the horizontal projection length of the bending tube. However this approximation is not valid for laminar flow as the flow velocity profile differs for straight and bending tubes.

Diffusional Deposition

Some particles will diffuse from high to low concentrations under Browninan motion. Taking particle concentration at the walls of the tube to be zero means that particles will diffuse towards them and be deposited, for laminar flow this can be modelled as [31]:

$$\eta_{\text{tube, diff}} = e^{\frac{-\pi dLV_{diff}}{Q}} = e^{-\xi Sh},$$

where V_{diff} is the deposition velocity for particle diffusion loss to the wall, Q is the volumetric flow rate through the tube and Sh is the Sherwood number. For laminar flow Holman [15] gives:

$$Sh = 3.66 + \frac{0.2672}{\xi + 0.10079\xi^{1/3}}$$
$$\xi = \frac{\pi DL}{Q},$$

and for turbulent flow Friedlander [9] gives:

$$Sh = 0.0118 \text{Re}^{7/8} Sc^{1/38}.$$

The laminar flow case is in very good agreement with the analytic solution created by Gormley and Kennedy [11] and the use of the turbulent flow equations is supported by Brockmann, McMurry and Liu [3].

Inertial Deposition in a Bend

Bends divert the direction of gas flow and hence particulates deviate from the flow due to inertia and become deposited on the wall of the tube bend. Crane and Evans [6] give a simple empirical correlation for the transport efficiency of particles undergoing a bend of 90° which can be extended to accomodate arbitrary angles as follows:

$$\eta_{\text{bend,inert}} = 1 - Stk(\vartheta),$$

where ϑ is the bend angle.

Further work by Cheng and Wang [5] and Pui et al. [23] indicates that for $Stk < 0.1$ there is no bend deposition. Pui et al. [23] also indicates that bend deposition for turbulent flows can also be expressed independantly of Re as follows:

$$\eta_{\text{bend,inert}} = e^{-2.823Stk\vartheta}.$$

Function Varification

All of the equations used in the routines were checked against numerical and graphical examples in [31] and were found to be in excellent agreement. Occasionaly slight numerical differences were noted. These were always due to the nature of floating point calculations and the difference between the values of some constants (such as the absolute gas viscosity of air) used.

Fieldwork

At Cranfield Airport we would collect data from 8 take-offs and landings of the FAAM aircraft[9]. In particular we were interesed in tyre smoke emissions on landing.

3 Experimentation

Sampling Systems for Cranfield

Basic inlets were designed for four different aerosol sampling instruments (table 1). These in-

---

[9]A modified BAE 146 airplane.

struments would be used in a field experiment attempting to measure the size distribution and quantity of aerosol particulates given off from airplane tires in landings. The field work would be undertaken at Cranfield Airport and would be the first practical test of the SPARCLE instrument designed and built in-house in the AOPP Department, Oxford. In my calculations the following basic assumptions were made:

Table 1: Sampling Instruments

Instrument	Tube Diameter	Flow Rate
SPARCLE	3.2 mm	25 ml/min
CPC	6 mm	300 ml/min
		1500 ml/min
OPC	3.2 mm	1000 ml/min
	6 mm	
APS	3.2 mm	2000 ml/min
	6 mm	

sumptions were made:

- Experiments would be conducted at STP, small daily variations in temperature and pressure have little effect on the efficiency of the system

- Calculations prior to the field test assume a wind speed of between $4 \, \mathrm{cms}^{-1}$ and $6 \, \mathrm{cms}^{-1}$ based on MET office data, actual windspeed data was collected on the day of the experiments and then used for new efficiency curves

- There would be either one or two 90° bends in the tubing

- Preliminary calculations assume $3 \, \mathrm{m}$ of tubing would be used

- Inlet lengths are similar in magnitude to inlet diameters

As previously noted, many of the functions used have well defined limits over which they have been tested. Users of the packages I have created should be aware of these limits when using the routines.

Upon performing multiple sets of efficiency calculations it became clear that the principle sources of losses for particles larger than 1 micrometer were from gravitational settling, bend deposition and inlet losses whereas particulates smaller than 0.01 micrometers are mainly lost through diffusional deposition (see figure 2).
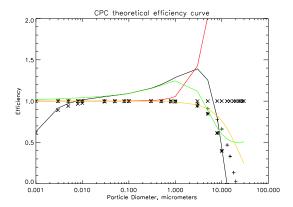

Figure 2: Theoretical efficiency curve for the CPC inlet where $U_0 = 400 \, \mathrm{cms}^{-1}$, horizontal tube length is $20 \, \mathrm{cm}$, total tube length is $150 \, \mathrm{cm}$, tube diameter is $3.2 \, \mathrm{mm}$ and there is one 90° bend. Efficiency as follows: + = gravitational settling in tube, * = bend deposition, X = inertial deposition in tube, red=aspiriational efficiency of the inlet, yellow=gravitational settling in the inlet, green=inertial deposition in the inlet.

An efficiency > 1 indicates that particulates are preferentially drawn into the inlet and thus are oversampled. This generally occurs for high ambient air flow velocities and particles larger than 1 micrometer in diameter. This gain can counteract the sharp inertial bend deposition losses and gravitational deposition over horizontal tube lengths over the size range $1 \, \mu\mathrm{m}$ to $20 \, \mu\mathrm{m}$.

Based on my calculations I designed a series of inlets which minimised particulate losses. These consisted of $1.5 \, \mathrm{m}$ of tubing (of which $20 \, \mathrm{cm}$ was horizontal), $3.2 \, \mathrm{mm}$ in diameter. There was a single 90° bend to facilitate isoaxial sampling.

SPARCLE has a much lower flow rate than the other instruments which significantly limits the ef-

6

ficiency of the sampling system. Two possible solutions to the problem were:

- Increase SPARCLEs flow rate - a difficult proposition given the relatively tight schedule being worked to.

- Decrease inlet diameter - although this would have the effect of increasing inlet velocity it would adversely affect other components of the efficiency equations having little net overall effect. Also, on a practical level, significantly decreasing inlet diameter would mean using metal rather than flexi-plastic tubing. This would be impractical as we anticipated needing to make alterations to the inlet systems on an ad-hoc basis at Cranfield.

Due to these considerations it was decided to keep my original design for the SPARCLE inlet and keep the low flow rate problem in mind for the future.
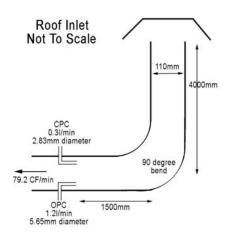
Roof Sub-sampling Inlet

Figure 3: Diagram of sub-sampling inlet system on the roof of the Atmospheric Physics building.

Figure 3 is a schematic of the sub-sampling system on the roof of the atmospheric physics building. It was last used to collect data on bonfire night 2007 with the CPC and OPC instruments.

The sub-sampler incorporates a vertical tube with hood, which prevents large foreign particles (such as rain, sleet, leaves etc.) from entering the inlet. For accurate analysis of the system extensive fluid dynamics modelling would need to be performed on the flow around the inlet. Based on information from several papers [21; 5] I made a simple model of the efficiency of the inlet:

$$\eta_{system} = \eta_{\text{inl}} * \eta_{\text{tube}} * \eta_{\text{cap}},$$

where $\eta_{\text{cap}} = \eta_{\text{bend}}$ for a bend of 110°. An approximation of the angle through which particulates must turn to enter the inlet. The efficiencies of the OPC and CPC instruments were then calculated based on flow rates in the sub sampling system and a complete efficiency curve for the total system was drawn up (see figure 4). These can be used to analyse data collected on bonfire night 2007.
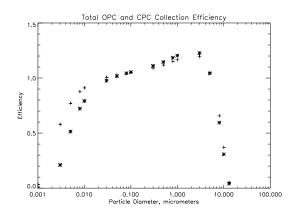

Figure 4: Efficiency curves for the OPC and CPC when sampling from the roof subsampler with outside air speed of $300 \, \text{cms}^{-1}$. + = OPC and * = CPC

Cranfield Fieldwork

Figure 5 shows our setup on the airfield. Space constraints meant we did not use the APS. Continuos data sets were taken for OPC, CPC and SPARCLE. Times of interest (take offs, landings etc) were noted.
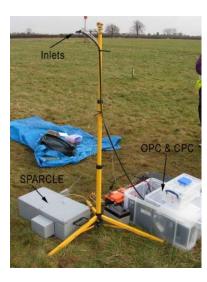
Figure 5: Instrument and inlet setup at Cranfield. Inlets are pointing into the wind and are isoaxial. Instruments are approximately $50\,\mathrm{m}$ down wind of aircraft landing area.
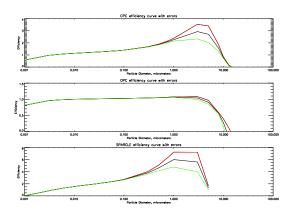

Figure 6: Error Graphs for each instrument. Red indicates upper error bound and green indicates lower error bound. Black is the calculated efficiency for the set up using mean windspeed for the day

Meteorological data for the day was supplied by the Manchester LIDAR team. I created a programme to read this data in, check for incorrect values and remove them (the LIDAR team experienced problems on the day in the form of power spikes which would show up as bad data - in the case of wind speed this would manifest as very low or negative values). The fluctuation of the wind was treated as a random error in the calculations which affects the precision of the efficiency calculations. I used a Monte Carlo error analysis method to generate error envelopes which surround the efficiency curves. Figure 6 these envelopes.

My colleague and I created functions which converted instrument data into a useful form for our purposes. This was done either directly from raw instrument data or by making use of functions provided by our supervisor.

When at Cranfield photographs were used to document the aircraft takeoff and landing. Tyre smoke on landing was only briefly observed on one sortie suggesting there was little aerosol tyre smoke for our instruments to pick up. We also recorded the times when we smelt either burning fuel or rubber. These were then used as event markers in data analysis (for an example see figure 7). Each instrument has a delay between a par-
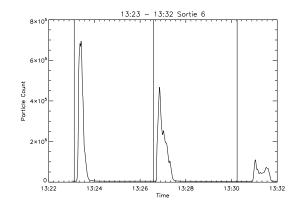

Figure 7: CPC data for sortie 6. Particle count is in count per cc. Vertical lines indicate times either kerosene or rubber was smelt, the first being just after taxiing past, second after takeoff, third after landing. The double peak is due to vortices spilling off the wing of the plane on landing.

ticle entering the inlet and arriving at the detector as detailed in table 2. This must be taken into account when looking for data peaks corresponding to events.

Figure 7 is typical of the CPC data and it shows that the aerosol particle count is significantly in-

Table 2: Instrument delays

Instrument	Flow Speed	Tube Length	Delay
SPARCLE	5.2 cm/s	155.5 cm	30 s
CPC	17.7 cm/s	221.5 cm	12.5 s
OPC	207.2 cm/s	151.5 cm	0.7 s

creased when the aircraft taxis, takes off or lands. This is most likely due to the combustion products ejected from the engines.

The CPC data gives no particulate size information. The double peak was originally thought to be tyre smoke emissions from the two separate landings of back and front tyres. This was cross checked with LIDAR data which showed almost no tyre smoke emission over the whole day. It is now thought that the double peak is caused by vorticies spilling off the back of the wings on landing which disrupts the flow of the ejected combustion products.

SPARCLE records details of events and the time elapsed between events[10]. When this happens the phase function of the particle is measured using a laser and multiple CCDs. We created a function to interpret the SPARCLE data in two different ways:

- The number of events are binned in user defined intervals (20 s initially) to produce a smoothed data set with similar function to that of the CPC (see figure 8).

- The signal registered by the CCDs was summed for each event and then again binned in user defined intervals. This gives weighting to particles of larger size as they will have a phase function containing more data than smaller particles.

Both data sets are too noisy to gain any useful information from. This suggests that the combustion products are not picked up over the size range which SPARCLE measures.

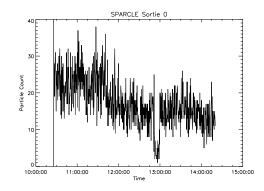[10]An event is defined as a particle entering the detector.

Figure 8: Smoothed SPARCLE event count data over the day. The sudden drop around 12:50 is due to a zero filter placed over the inlet for 10 minutes.
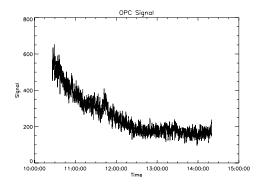

Figure 9: Smoothed OPC event count data over the day.

The OPC measures events per second within a range of size bins[11]. We created a function to sum the data in the bins for each time stamp and then smoothed the result by convolving it with a top hat function of width 20 s. Again it trainspired that over the range of particle sizes being measured by the OPC there is too much background noise to derive useful information. However, looking at the signal for the entire day for both OPC and SPARCLE (see figures 8 and 9 shows that the two broadly agree with each other as to the trend in background noise - observations in the afternoon (which was much less cloudy than the morning) have less background noise than those in the morning due to less ambient aerosol.

---

[11]Size bins in micrometers: 2-3, 3-4, 4-5, 5-7.5, 7.5-10, 10-15, 15-20, >20

9

4 Conclusion

The inlet designs for the CPC and OPC were sufficient to observe aerosol particulates smaller then $10\,\mu$m at the Cranfield tests. This can be explicitly seen in figure 10 which shows that the cut off of the system is significantly greater than the size of the bulk of the particles observed on the day. This can not be shown explicitly for the CPC as it does not record size data. However the strong signal observed each time the plane passes implies that there were no inlet problems. The inlet for SPARCLE was insufficient for the required measurements as the efficiency cut off of the system is around $5um$ (see figure 6). Before being used again a completely new inlet should be designed. The main cause of the low cut off and sizeable oversampling was the ratio U_0/U which was very large. Possible fixes for this problem have already been discussed but a better solution would be to design a sub-sampling system not dissimilar to that on the roof of the Atmospheric Physics building (see figure 3). This, combined with varying the diameters of the inlets, could be used for all instruments for isoaxial and isokinetic sampling conditions. This would make instrument set up more complicated as a sub sampling system is likley to be bulky.

Further Work

Further analysis of Cranfield data.

The calculated efficiencies of the sampling systems can be used to perform more careful analysis of the Cranfield data. For the CPC this would involve determining an average efficiency for the system as the data is not binned by size. Then, using a Monte Carlo approach, errors could be calculated for the data.

A similar approach would be used with SPARCLE as it also does not bin data according to size. For a more detailed analysis the phase function of each event could be analysed and size data determined. This would allow more detailed conclusions to be drawn about the size distributions of aerosols measured as the severe oversampling of particles between $0.1\,\mu$m and $3\,\mu$m in diameter would be accounted for.

Modelling the fluid dynamics of an inlet.

To more accurately calculate the efficiencies of aerosol inlets the fluid dynamics of the airflow should be modelled. This can be achieved with a simple model which can be extended to more complicated cases (such as the inlet of a sub-sampling system).

As a starting point the sampling efficiency of a simple cylindrical inlet could be modelled using a two dimensional rectangular grid with the upper and lower edges of the grid representing the walls. Start with a fixed distribution of particulates at one end and, column by column model their motion horizontally through the grid by calculating the total force on the particle at each step. The calculations would need to include gravity, inertial forces, a parabolic flow distribution and Brownian motion. Particles which exit the grid at the upper and lower bound are considered to have been deposited on the walls and are lost. The number of particles which arrive at the other end of the grid as a fraction of the original total is a measure of the efficiency of the inlet. This concept can be extended by introducing different flow distributions and different shaped grids.
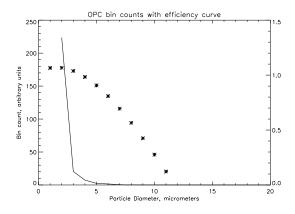

Figure 10: OPC total bin counts in arbitrary units with overlayed efficiency curve. — = OPC bin data, * = efficiency curve. Right side y axis is efficiency.

References

[1] SP Belyaev and LM Levin. Investigation of aerosol aspiration by photographing particle tracks under flash illumination. *J. Aerosol Sci*, 3:127–140, 1972.

[2] SP Belyaev and LM Levin. Techniques for collection of representative aerosol samples. *J. Aerosol Sci*, 5:325–338, 1974.

[3] JE Brockmann, PH McMurry, and BYH Liu. On simultaneous coagulation and diffusional loss of free molecule aerosols in turbulent pipe flow. *Aerosol Science and Technology*, 1(2):163–178, 1982.

[4] RJ Charlson, SE Schwartz, JM Hales, RD Cess, JA Coakley, JE Hansen, and DJ Hofmann. Climate forcing by anthropogenic aerosols. *Science*, 255(5043):423–430, 1992.

[5] YS Cheng and CS Wang. Motion of particles in bends of circular pipes. *Atmospheric Environment (1967)*, 15(3):301–306, 1981.

[6] RI Crane and RL Evans. Inertial deposition of particles in a bent pipe. *J. Aerosol Sci*, 8:161–170, 1977.

[7] CN Davies and M. Subari. Aspiration above wind velocity of aerosols with thin-walled nozzles facing and at right angles to the wind direction. *J. Aerosol Sci*, 13(1):59–71, 1982.

[8] MD Durham and DA Lundgren. Evaluation of aerosol aspiration efficiency as a function of Stokes number, velocity ratio and nozzle angle. *J. Aerosol Sci*, 11:179–188, 1980.

[9] S.K. Friedlander. Smoke, dust, and haze: Fundamentals of aerosol behavior. *New York, Wiley-Interscience, 1977. 333 p.*, 1977.

[10] NA Fuchs and RE Daisley. The mechanics of aerosols. 1964.

[11] PG Gormley and M. Kennedy. Diffusion from a stream flowing through a cylindrical tube. In *Proc. Royal Irish Acad*, volume 52, pages 163–169, 1949.

[12] H. Granek, J. Gras, and D. Paterson. Particle transmission efficiecny of the Cape Grim 10-m sampling inlet. *Baseline Atmospheric Program Australia 1999-2000*, page 18.

[13] SA Grinshpun, GN Lipatov, and TI Semenyuk. A study of sampling of aerosol particles from calm air into thin-walled cylindrical probes. *J. Aerosol Sci*, 20:1561–1564, 1989.

[14] J. Heyder and J. Gebhart. Gravitational deposition of particles from laminar aerosol flow through inclined circular tubes. *J. Aerosol Sci*, 6:311–328, 1977.

[15] JP Holman, PE Jenkins, and FG Sullivan. Experiments on individual droplet heat transfer rates. *International Journal of Heat and Mass Transfer*, 15:1489–1495, 1972.

[16] HT Kim, YJ Kim, and KW Lee. New PM 10 inlet design and evaluation. *Aerosol science and technology*, 29(4):350–354, 1998.

[17] AB Laktionov. Aspiration of an aerosol into a vertical tube horn a flow transverse to it. *Fiz. Aerozoley*, 7:83–87, 1973.

[18] GN Lipatov, SA Grinspun, GL Shingaryov, and AG Sutugin. Aspiration of coarse aerosol by a thin-walled sampler. *Journal of aerosol science*, 17(5):763–769, 1986.

[19] BYH Liu, ZQ Zhang, and TH Kuehn. A numerical study of inertial errors in anisokinetic sampling. *Journal of Aerosol Science*, 20(3):367–380, 1989.

[20] K. Okazaki, R.W. Wiener, and K. Willeke. Non-isoaxial aerosol sampling: Mechanisms controlling the overall sampling efficiency. *Environ. Sci. Technol*, 21(2):183–187, 1987.

[21] T.M. Peters and D. Leith. Concentration measurement and counting efficiency of the aerodynamic particle sizer 3321. *Journal of Aerosol Science*, 34(5):627–634, 2003.

[22] J. Pich. Theory of gravitational deposition of particles from laminar flows in channels. *J. Aerosol Sci*, 3:351–361, 1972.

[23] DYH Pui, F. Romay-Novas, and BYH Liu. Experimental study of particle deposition in bends of circular cross section. *Aerosol Science & Technology*, 7(3):301–315, 1987.

[24] PG Saffman. The lift on a small sphere in a shear flow. *J. Fluid Mech*, 22:385–400, 1965.

[25] PG Saffman. The lift on a small sphere in a slow shear flow-corrigendum. *J. Fluid Mech*, 31:624, 1968.

[26] SK Satheesh and K. Krishna Moorthy. Radiative effects of natural aerosols: A review. *Atmospheric Environment*, 39(11):2089–2110, 2005.

[27] H. Schlichting. Author Boundary-layer theory/Trans. by J. Kestin. *New York: McGraw-Hill, 1968.*, 1968.

[28] LC Schwendiman, GE Stegen, and JA Glissmeyer. Methods and aids for assessing particle losses in sampling lines. In *American industrial hygiene conference*, volume 1, 1975.

[29] J.W. Thomas. Air Pollut. 1958.

[30] E. Vincent. Mark 1985. JH Vincent, PC Emmett and D. Mark, The effects of turbulence on the entry of airborne particles into a blunt dust sampler. *Aerosol Science and Technology*, 4:17–29, 1985.

[31] K. Willeke and P.A. Baron. *Aerosol measurement: principles, techniques, and applications*. Van Nostrand Reinhold New York, 1993.

[32] K. WILLEKE and S. HANGAL. Overall efficiency of tubular inlets sampling at 0 to 90 degrees from aerosol flows. In *Aerosols: Science, Industry, Health, and Environment: Proceedings of the Third International Aerosol Conference, September 24-27, 1990, Kyoto International Conference Hall, Kyoto, Japan*, page 355. Pergamon, 1990.

[33] N. Yamano and JE Brockmann. Aerosol Sampling and Transport Efficiency Calculation (ASTEC) and Application to Surtsey/DCH Aerosol Sampling System, Sandia National Laboratories. Technical report, NUREG/CR-5252 SAND88-1447 R3, 1989.